International Journal of Progressive Sciences and Technologies (IJPSAT)
ISSN: 2509-0119.

Vol. 45 No. 1 June 2024, pp. 224-239

# *The Real–Time Flipping Dynamics Studies of Dipolar Diflourophenylene Rotator (Compass Needle) of Crystalline Siloxaalkane Molecular Compass*

Prof. Dr. Anant Babu Marahatta[1,*]

[1]Professor of Chemistry, Engineering Chemistry and Applied Science Research Unit, Department of Civil, Computer and Electronics Engineering, Kathford Int'l College of Engineering and Management (Affiliated to Tribhuvan University), Kathford Int'l Education & Research Foundation, Lalitpur, Nepal
*Corresponding author: abmarahatta@gmail.com/anant.marahatta@kathford.edu.np



**Abstract – One of the most indispensable strategies of nanotechnology is to integrate the networks of molecular arrays and their explicit functionalizable physicochemical properties of those type crystalline materials that exhibit unique amphidynamic behavior at wide range temperature regimes, and respond genuinely to the external stimuli owing to the inventions of smart, and intelligent nanomachines. The recently synthesized macroscopic compass like macrocyclic crystalline compound with a completely closed structural topology possessing a Si–C spin axis, and a dipolar diflourophenylene (rotator) ring encapsulated into the peripheral –(Si–O)$_x$– & –Si–O–Si– made siloxaalkane spokes (stator) is one of such type materials whose central rotator is experimentally observed as 1π-flipped in two degenerate positions ($\beta$ and $\beta'$) at T = 273 K. Herein, all the associated rotary dynamical assets of this gyrotop molecular arrays are probed under crystalline conditions by employing the NCC–DFTB/MD simulation scheme. The general results achieved in this study are found to justify the X–ray/$^1$H–NMR predicted flipping motions and temporal behavior of the central dipolar rotator in real-time scales. When the average kinetic temperatures T of the molecular ensemble are set to 1200 K & 600 K, the rotator is found to consume ≅8 ps & ≅45 ps with the flipping rates of $\kappa_1$ = 0.022 ps$^{-1}$ & $\kappa_2$ = 0.125 ps$^{-1}$ respectively for the specific $\beta \rightarrow \beta'$ 1π-flipping, but when T is reduced to 273 K, this flipping motion is completely forbidden within the present simulation timeframe of ≤ 200 ps. The flipping barrier value $E_a$ = 4.3 kcal/mol obtained from the Arrhenius equation is also found to lie in well agreeable range to that determined through the *Gaussian–external* PES techniques ($E_a$ = 4.9 kcal/mol). The results presented here are quite essential to understand the compass/gyroscope like functions of the siloxaalkane molecular analogues which in turn speculate their functionalizing masterplans comprehensively.**

**Keywords – MD Simulation, Nanomachines, Amphidynamic Materials, Flipping Motions/Rates/Barriers**

## 1. INTRODUCTION

Over the last decades, the crystalline macrocyclic molecular compounds with bridged π–electron systems have received much attentions because of their unique structures, contrasting internal dynamics, and promising functionalizable physicochemical properties [1–5]. In particular, the crystalline phenylene bridged supramolecular macrocages with the axial Si–C spin axes, a central non–polar (phenylene ring) or polar rotary unit (substituted phenylene ring), and the peripheral –(Si–O)$_x$– &–Si–O–Si– segments made static siloxaalkane spokes (Scheme 1) are expected to possess various state-of-art amphidynamic properties owing to their direct utilizations/ employments in inventing and advancing various Nano technological and molecular machinery attributes [1–4]. Based on the collective working mechanisms of their explicit spare parts and the integrative amphidynamic behaviors of their molecular arrays, these special type crystalline molecular analogues are more typically recognized as molecular compass (the rotating unit is a substituted phenylene ring (dipolar)) and molecular gyroscope (the rotating unit is a non-substituted phenylene ring (nonpolar)) (encircled in Scheme 1) in the nanometric world. These molecular arrays explicitly behave quite analogous to the macroscopic compass and gyroscope both internally and externally in the crystalline state [5]. Several experimental/theoretical

investigations and molecular internal dynamics probing techniques have already confirmed their crystal structures and crystallinities, and the facile rotary dynamics of their central rotator in respect to the peripheral stationary spokes at high to moderate temperature regimes [3–12] along with the explicit discloses of the architecting strategies of the gyrotop molecules and their rotary dynamics probing descriptors [1, 2, 12–15]. The present author himself has reported the in–depth structural characterizations of such type amphidynamic molecular arrays under both crystalline and non-crystalline conditions with and without addressing their predominant type van der Waals dispersive forces through which the entire molecular assemblies in the crystalline state are bound [1,2,12–15].

In the computational/experimental molecular model/prototype designing strategies and the artificial molecular machines tailoring mainstream research fields, the custom syntheses play very crucial roles by enabling the chemists to design the specific type solid state gyrotop molecules such as molecular gyroscope/compass systems with the effective control over rotators' surrounding space (free–volume unit) and flipping energy barrier $E_a$ [3, 4]. The same type solid–state engineering and architecting strategies led the prominent research groups of Setaka et al. to accomplish the complete synthesis of the crystalline siloxaalkane (a) molecular gyroscope with a nonpolar phenylene rotator (hereafter, ROT–2H), and (b) molecular compass with a dipolar diflourophenylene rotator (hereafter, ROT–2F) by adopting the perfectly closed structural topologies (Scheme 1); a mandatory molecular morphology required to attain a gyrotop molecule in terms of exhibiting specific gyroscopic/compass like functions genuinely. They designed and synthesized experimentally the both ROT–2H and ROT–2F type macrocages separately without changing the surrounding stationary siloxaalkane frameworks and the axial Si–C spin axis, but with replacing the central rotary phenylene unit of the former by dipolar diflourophenylene (compass needle) in the latter (Scheme 1). Experimentally, they observed the promising collective effects and cumulative properties such as dichroism and birefringence of both of these siloxaalkane molecular analogues in their crystalline phases [8–10] that are ambiguously believed to be functionalized explicitly in optics as dichroic/birefringent materials. More especially, the change in "dielectric properties" of the ROT–2F's dipolar diflourophenylene rotator observed by them is recognizably remarkable as it tuned the possibility of controlling internal rotary motions through the usage of external stimuli, and hence nominated this crystalline molecular compass as the most promising dielectric materials. Additionally, the absolute inclusions of the electronegative O atoms on the three explicit peripheral siloxaalkane arms of the both ROT–2H and ROT–2F, the complete presence of the robust type $-(Si-O)_x-$ & –Si–O–Si– segments in them, and the distinctive electronegativity differences between the Si and O atoms with intense polar Si–O bonds, etc. features have facilitated their rational applications in the molecular machinery world. All these applicative attributes are already presented demonstratively, and verified experimentally/ theoretically in molecular level elsewhere [1,8–10,12] where the most diligent dynamical phenomena associated with the crystalline ROT–2H and ROT–2F are pointed out on the basis of which the facile 1π phenylene flipping with three stable positions at temperature $T \geq 223K$ [8] of the former and the relatively more constrained 1π diflourophenylene flipping with two stable yet degenerate positions (designated as $\beta$ and $\beta'$) at T = 273K [9] of the latter are stressfully explained. These experimental characterizations and rotary flipping dynamics were materialized by the research groups led by H. Kono, and the present author himself by employing several theoretical/ computational quantum mechanical means (*ab initio* DFT, non-self-consistent-charge (NCC) –, and self-consistent-charge (SCC) – density-functional based tight-binding (DFTB) schemes plus their extended features aligned to the solid state crystalline systems, and *Gaussian* interface assessing external programs "*Gaussian–external*" methodology), and disclosed the exclusive molecular packing structures and rotary dynamics of the both ROT–2H and ROT–2F crystalline systems [1, 2, 12–16]. All the theoretically derived structural and dynamical assets of the ROT–2H were found to be quite consistent to the experimental observations reported by Setaka *et al.* elsewhere [8, 9]. And, most of the experimentally unrevealed yet impossible type dynamical attributes such as real time flipping motions, flipping dynamics, temporal rotary motions, and the associated flipping energy barriers $E_a$ between all the intermittent rotary positions, etc. of the ROT– 2H molecular gyroscope predicted by either of the NCC– / SCC– DFTB molecular dynamics (MD) methods stood as the strongest evidences for verifying all those experimental reports. But, the similar type NCC–DFTB/MD based investigations concentrated into the crystalline ROT–2F molecular compass system were not reported earlier, which in fact are equally indispensable to understand it's internal flipping dynamics in real-time scales, and to verify the experimentally observed degenerate 1π-flipping motions. Herein, the NCC–DFTB/MD produced theoretical interpretations at wide ranged kinetic temperature regimes (T = 1200K, 600K, 300K, 273K) aimed to elucidate the rotary dynamics of the dipolar diflourophenylene rotator of the ROT–2F molecular compass under crystalline conditions (herewith, periodic boundary condition, PBC) are presented. Being the current ROT–2F crystalline molecular systems extremely giant (number of molecules per unit cell

= 4; and number of atoms per molecule = 195) that makes the DFTB+ simulation parser codes computationally complex, the DFTB+ inclusive with van der Waals dispersions model (Slater Kirkwood model [17]) codes are excluded in the NCC–DFTB/MD simulation. The detailed dynamical assets conferred herewith are the most imperative means to materialize the overwhelming concepts associated with (a) functionalizing principles of the dielectric nanomaterials, (b) typical working and functionalizing mechanisms of the crystalline dipolar molecular rotors (entire molecular assembly), (c) macroscopic compass like functions of its dipolar molecular analogue quantitatively, (d) temperature dependent picosecond rotary dynamics of the dipolar rotary segment and its tentative lifespans at each intermittent rotary positions, (e) induced internal energy of the crystalline molecular arrays required to overcome the flipping energy barrier $E_a$, (f) temperature dependent flipping kinetics, etc. of the amphidynamic crystalline molecular compass. This research article is structured as: in section 2; Computational Detail, in section 3; Result and Discussion, in section 4; Summary and Conclusion are presented.

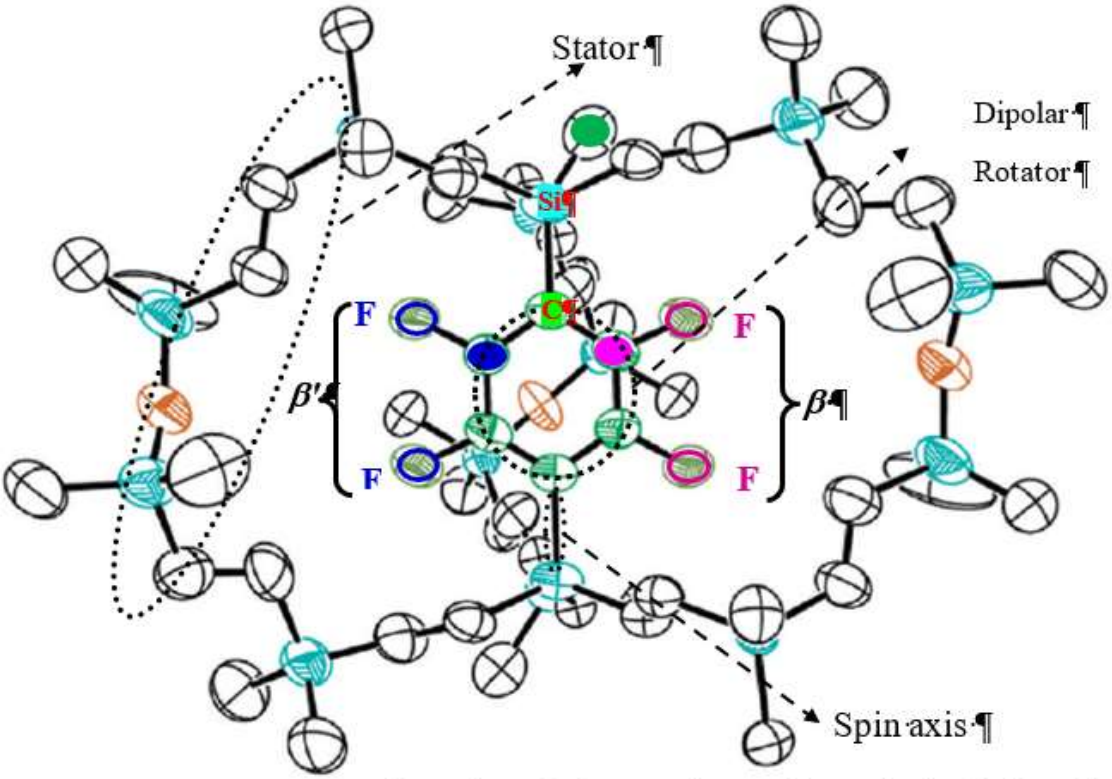


**Scheme 1.** An X–ray crystallography of the experimentally synthesized siloxaalkane molecular compass with two degenerate stable positions of diflourophenylene rotator (compass needle). The dihedral angle used to locate its stable angular positions in the MD derived rotational trajectory is defined by the spin axis (Si–C bond), the C atom next to the Si atom in a siloxaalkane spoke (green spheroid), and the *ortho* C atom in a rotator (other colored spheroids). The pink and blue spheroids represent the *ortho* C atoms for the two X–ray observed stable positions $\beta = 0.56\pi$, and $\beta' = 1.57\pi$ respectively. Hydrogen atoms are omitted for clarity.

## 2. COMPUTATIONAL DETAIL

Out of the two experimentally observed degenerate stable positions B (diflourophenylene angular position (dihedral angle $\phi$ = 0.56π) = $\beta$ ) and B' (diflourophenylene angular position (dihedral angle $\phi$ = 1.57π) =$\beta'$ ) of the crystalline siloxaalkane molecular compass ROT−2F (occupancy factors ratio 0.50:0.50), the NCC−DFTB optimized Cartesian atomic coordinates of the unit−cell (equilibrium nuclear positions of each atom) of the former structure (dihedral angle $\phi$ = 0.44π) were taken here as the NCC−DFTB/MD simulation trial geometry. The crystallographic information such as crystal lattice, and unit−cell parameters (lattice vectors) *a*, *b*, & *c*, and the angles between them $\alpha$, $\beta$, & $\gamma$ of the concerned structure required to incorporate its entire molecular arrays computationally were extracted from the X−ray produced *.cif* extended files. The initial velocities of every atomic nuclei of its unit−cell were generated from the '*VelocityVerlet{}*' random seeding techniques so that the quantum mechanical requirements of the DFTB+ simulation parser codes were met precisely for satisfying the mean kinetic temperature T. The velocity Verlet algorithm [18] driver was called for propagating the atomic motions of every nuclei (velocity Verlet dynamics): each concerned velocities and positions of every atomic nuclei were computed at each MD step *i* while the simulation trajectories were on the fly with the time increment of $\Delta t$ = 0.2 fs for the total time duration of ~300 ps. The explicit NCC−DFTB/MD simulation codes at each specific kinetic temperatures T (T = 1200 K, 600 K, 300 K, and 273 K) were run at constant energy without any thermostating and barostating parameters so that the typical NVE ensemble was achieved throughout the entire computational procedure. Being the low kinetic temperature simulations computationally tedious and time consuming, the specific MD trajectories run at T = 300 K and T = 273 K were terminated manually at the time scale of ~160 ps. The general DFTB+/ MD simulation parser coding tags such as 'MovedAtoms', 'OutputPrefix', 'MDRestartFrequency', 'ConvergentForcesOnly', and 'Effective Temperature', etc. [19] were promptly executed in order to ensure the (a) complete movement of all the atomic nuclei, (b) prefixing of the recurrent geometry files, (c) periodical rewriting of the nuclear positions (geometry) and velocities in the *.xyz* extended geometry file, (d) controlling of the prematurely stopped dynamics, and (e) specific representation of the mean kinetic temperature of the simulating ensemble, etc. respectively. The specific dihedral angle $\phi$ of the central diflourophenylene rotator (the complete definition of $\phi$ is mentioned in the caption of Scheme 1) required to depict its rotary trajectory at each T, and to inspect its temperature dependent rotary motion was determined for each recurrent MD step geometry, and its temporal behavior (flipping dynamics) was investigated in real−time scales. Since the present author was unable to run many MD trajectories not only due to being the current simulation systems computationally giant but also due to the unavailability of sufficient computational resources, no average ensemble was able to take in the present analyses. Therefore, all the temperature dependent rotary dynamics were determined based on the few trajectories run with the dissimilar initial velocities at each kinetic temperature T.

## 3. RESULT AND DISCUSSION

### 3.1 Rotary Dynamics Associated Datasets of the Diflourophenylene Rotator

The ground state electronic structures of the two degenerate molecular structures B and B' of the present crystalline siloxaalkane molecular compass ROT−2F were already confirmed by the present author and his collaborators via the both theoretical (*Th.*) and experimental (*Expt.*) techniques whose respective diflourophenylene positions are designated herewith as $\beta$ and $\beta'$ interrelated to each other by complete 1π flipping. According to the research articles reported by us elsewhere [1, 2, 9], the specific dihedral angles $\phi$ deterministic to their internal flipping motions (positions) of the diflourophenylene occurred inside the static siloxaalkane spokes are converged to *Th.* 0.44π (*Expt.* 0.56π) and *Th.* 1.44π (*Expt.* 1.57π) respectively. Therewith, the dihedral angle $\phi$ that quantifies these specific angular positions was defined by the priory selection of the particular atomic positions of the static siloxaalkane arms (the complete definition of $\phi$ is given in scheme 1). The exactly same definition of the $\phi$ is programmatically implemented herewith in the course of verifying these 1π−flipped positions (B↔B' (or $\beta \leftrightarrow \beta'$)) in real time scale: all the MD derived trajectories at different kinetic temperatures T (T = 1200 K, 600 K, 300 K, and 273 K) were analyzed explicitly, and the specific value of the $\phi$ was retrieved with respect to the simulation timescale. Additionally, the *Gaussian−External* methodology (Method: "NCC−DFTB"; Interface: *Gaussian*; Driving strategy: '*External*' scheme of the *Gaussian* software; Mediator: *Python script*) produced flipping energy barrier

(activation energy barrier) $E_a$ for the B↔B' (or $\beta \leftrightarrow \beta'$) is 4.9 kcal/ mol. (Figure 1) as per the present author's report available elsewhere [1]: it is the exact energy barrier that is supposed to be overcome by the central dipolar diflourophenylene (compass needle) rotating unit of the present molecular compass while exhibiting complete 1π flipping motion internally under crystalline conditions. In the present MD simulation, the same magnitude of the $E_a$ is referred time to time; more especially while justifying the low-temperature (T = 300 K, & 273 K) flipping trajectories of the diflourophenylene rotator and its inability of undergoing complete 1π rotary motions within the viable MD simulation timeframe set throughout this study. Besides these rotary descriptors and the closely dependable variables deterministic to the notable rotary dynamics, the free–volume unit (each set of $d_{CO}$ $\{d_1, d_2, d_3\}$ (Å) = distance between the O atom of each siloxaalkane arm and the C atom of the central rotator) that quantitatively approximates the available space present around the rotary segment or depicts the void space left inside the siloxaalkane spokes in the time of

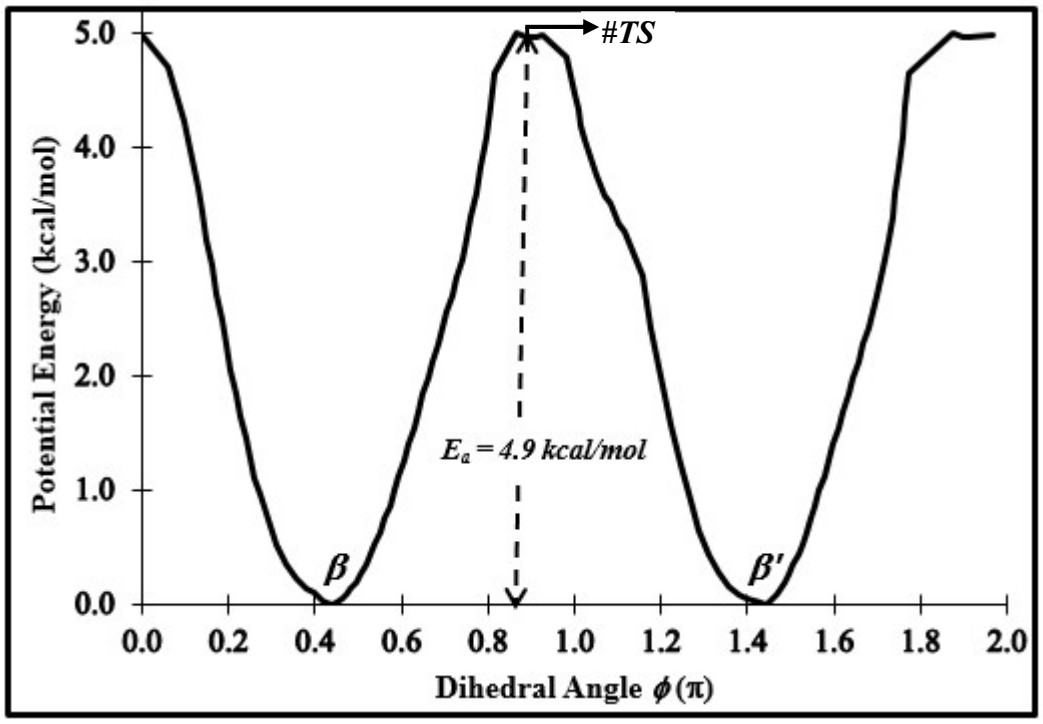


**Figure 1.** The NCC–DFTB derived rotational potential energy surface (PES) of the dipolar diflourophenylene rotator encapsulated centrally into the siloxaalkane cage of the molecular compass. The flipping barrier $E_a$ = 4.9 kcal/mol, and the two stable minima with 1π–flipped degenerate positions marked by $\beta$ and $\beta'$ at dihedral angle $\phi = 0.44\pi$ and $1.44\pi$ radians respectively are shown explicitly. This PES is reproduced from the original publication ref [1] of the same author for interpreting the NCC–DFTB/MD derived rotary trajectories (Figure 2–Figure5), and for quantizing the flipping motions of the rotator in real-time scales.

architecting the siloxaalkane gyrotops (prototype molecule of the molecular compass/gyroscope) at molecular level is also equally recognized as one of the most significant rotary parameters. In fact, the free–volume unit determines whether the rotary segment undergoes facile internal rotation with experiencing very nominal steric hindrance of the surrounding spokes or exhibits restricted flipping motions with bearing significant steric effects or is completely prevented from internal facile rotation. It can be justified by the set of the quantitative values of $d_{CO}$ $\{d_1, d_2, d_3\}$ (Å) (C = carbon atom of the rotator, and O = oxygen atom of the arm): the shorter $d_{CO}$ $\{d_1, d_2, d_3\}$ always specifies more constraints (more steric hindrance due to inward deformation of the peripheral

Si–O–Si made flexible siloxalakne arms) to the central rotating segment, and the longer $d_{CO}$ $\{d_1, d_2, d_3\}$ measures outward deformation or elongation of the same arms. Therefore, the proper analyses of the $d_{CO}$ datasets are indispensable in the course of interpreting MD predicted internal rotary dynamics and temperature dependent flipping rates of the central dipolar diflourophenylene segment in real-time scale. For the convenience of the readers/researchers, the complete "NCC–DFTB" derived $d_{CO}$ datasets responsible for quantizing the free–volume unit of each 1π flipped structures (B↔B' or $\beta \leftrightarrow \beta'$) are reproduced in Table 1. As per the experiences of the present author, these datasets are subjected to change significantly if the methodology is switched to "SCC–DFTB" with and without incorporating "Dispersion Energy Corrections" features [2]. But, for the current NCC–DFTB/MD simulation based studies, the SCC–DFTB derived $d_{CO}$ datasets are not useful at all, and hence excluded in Table 1.In fact, the successful implementations and employment of the SCC features of the DFTB+ via its MD formulation scheme was impracticable to the present simulation case due to the complexity of the crystal structures and their amphidynamic behaviors. The detailed impacts and correlations of all these explicit rotary descriptors in reference to the NCC–DFTB/MD produced internal rotary dynamics of the central dipolar diflourophenylene segment and the temperature dependent flipping kinetics at wide ranged average kinetic temperature regimes are explained in subsection 3.2.

Table 1. The "NCC–DFTB" derived rotary descriptors of the central dipolar diflourophenylene segment of the ROT–2F molecular compass

| Methods | Dihedral angle $\phi$ of the stable positions **Structure B ($\beta$) ↔ Structure B' ($\beta'$)** | | Free –Volume ($d_{CO}$ = $\{d_1, d_2, d_3\}$) (Å) | |
|---|---|---|---|---|
| | First ↔ 1π–flipped | $E_a$ (kcal/mol) | **Structure B** | **Structure B'** |
| X–ray | 0.56π ↔ 1.57π | – | 0.591,0.584,0.844 | 0.553, 0.579,0.859 |
| NCC–DFTB | 0.44π ↔ 1.44π | 4.9 | 0.589,0.589,0.844 | 0.589, 0.594,0.845 |

### 3.2 Real–Time Flipping Dynamics of the Dipolar Diflourophenylene Rotator

Usually, the DFTB+ geometry optimizer derived stable structures are consistent with the concerned equilibrium structures produced through its own MD simulation incorporated computational schemes: herewith, the NCC–DFTB optimizer run through the *Gaussian* PES scanning techniques (collectively called *Gaussian–external* methodology [1]) derived two stable flipping positions of the dipolar diflourophenylene rotator $\beta$ (structure B) and $\beta'$ (structure B'), and their respective dihedral angles $\phi$ deterministic to the alignment of the rotator centrally into the available free– volume unit of the siloxaalkane spokes are equivalent to the concerned structures/positions retrieved from the NCC–DFTB/MD produced trajectories. In this specific study, the complete 1π rotation between $\beta$ and $\beta'$ ($\beta \leftrightarrow \beta'$) plus their intermittent positions appeared in the several time dependent flipping courses (flipping MD-profiles) are traced out based on their angular stability and rotational PES depicted low energy global minima (Figure 1). Nevertheless, the opposite is also equally validated and implemented procedure: in this case, the NCC–DFTB/MD produced dihedral angle $\phi$ (π) of the most stable positions of the dipolar diflourophenylene rotator inspected on the concerned MD trajectories are used to quantize its temporal behavior in real time scale, and the NCC–DFTB optimizer (*Gaussian–external*) pinpointed global minima positions on the rotational PES are approved. In order to materialize these consequences quantitatively plus to theorize the flipping motions of the diflourophenylene rotator in real–time scales, and to reveal its closely associated picosecond rotary dynamics, its dihedral angles $\phi$ (π) determined at every consecutive MD step unit–cell geometry produced at each specific average kinetic temperature T = 1200 K, 600 K, 300 K, and 273 K are plotted with the real–time scales (ps) (Figure 2–Figure 5). The graphical representations of the time dependent angular variations (MD trajectories or temporal profiles) of it are explicitly shown at every average kinetic temperatures that were specifically selected based on the experimental observations reported earlier elsewhere [9] by Setaka *et al*. More particularly, the average kinetic temperatures T = 1200 K & 600 K were chosen just to reveal the experimentally impossible yet undetermined rotary dynamics of the rotator at relatively high temperature regimes, and the temperature T = 300 K & 273 K were implemented computationally mainly to examine whether the rotator exhibits facile flipping

through its Si–C spin axis by easy overcoming of the associated energy barrier $E_a$ = 4.9 kcal/mol. speculated on the rotational PES (Figure 1) (this barrier lies in between the two global minima $\beta$ and $\beta'$) or not when the internal average kinetic energy of the simulating ensemble is as equal as that of the room temperature ($T_{room}$ = 29 K). Beside this, the NCC–DFTB/MD derived rotational trajectories of the diflourophenylene (ROT–2F; molecular compass) and phenylene (ROT–2H; molecular gyroscope) rotators at T = 600K and 1200K (Figure 6 and Figure 7) for short timeframes of 20 ps and 15 ps respectively are also used here to compare their temporal flipping motions in real–time scales and to inspect the frequency of flipping while the size of the rotary segment is varied (phenylene: light rotator; diflourophenylene: bulky rotator). The concerned 20 ps and 15 ps long NCC–DFTB/MD derived trajectories of the crystalline ROT–2H molecular gyroscope were cropped from the pre-published datasets of the same author [12], and produced herewith. In order to mark the flipping sites of the diflourophenylene rotator clearly & demonstratively, and to depict its correct angular positions, the same representations such as $\beta$ and $\beta'$ mentioned in the concerned PES are referred in each time-dependent rotary profiles (Figure 2 to Figure 5). The exact angular positions deterministic to the initial and 1π–flipped states of the rotator are marked explicitly, and the complete simulating conditions of the ensembles are shown in each inset.

As illustrated diagrammatically in Figure 2, the diflourophenylene segment changes it's flipping angles with respect to the stationary peripheral siloxaalkane spokes within the stipulated timeframe of 200 ps when the internal kinetic temperature T of the ensemble is set to 1200 K. This rotating unit flips to the new position $\beta'$ (= 1.44π) from its original position $\beta$ (= 0.44π) after about 10 ps of its stay onto the latter. The average time that the rotator occupies on the $\beta'$ position is not less than 25 ps. Thereafter, the rotary profile shifts to the anticlockwise pathway, turns directly an angle of the magnitude 2π, and reaches to the degenerate $\beta'$ position ($\phi$ = ~ – 0.5π) where the rotator resides relatively longer time (~160 ps) before flipping back to the $\beta$ position ($\beta' \rightarrow \beta$) ($\phi$ = ~ – 1.5π) through the same direction. The net time consumed by the rotator while exhibiting a complete 1π $\beta \rightarrow \beta'$ rotation is found as equal as 8 ps. This rotary pathway with the frequent stable positions of the rotator at the particular angles $\beta$ and $\beta'$ confirms the PES scanning technique predicted angular positions of the global minima structures (Figure 1). Even though more frequent and instant

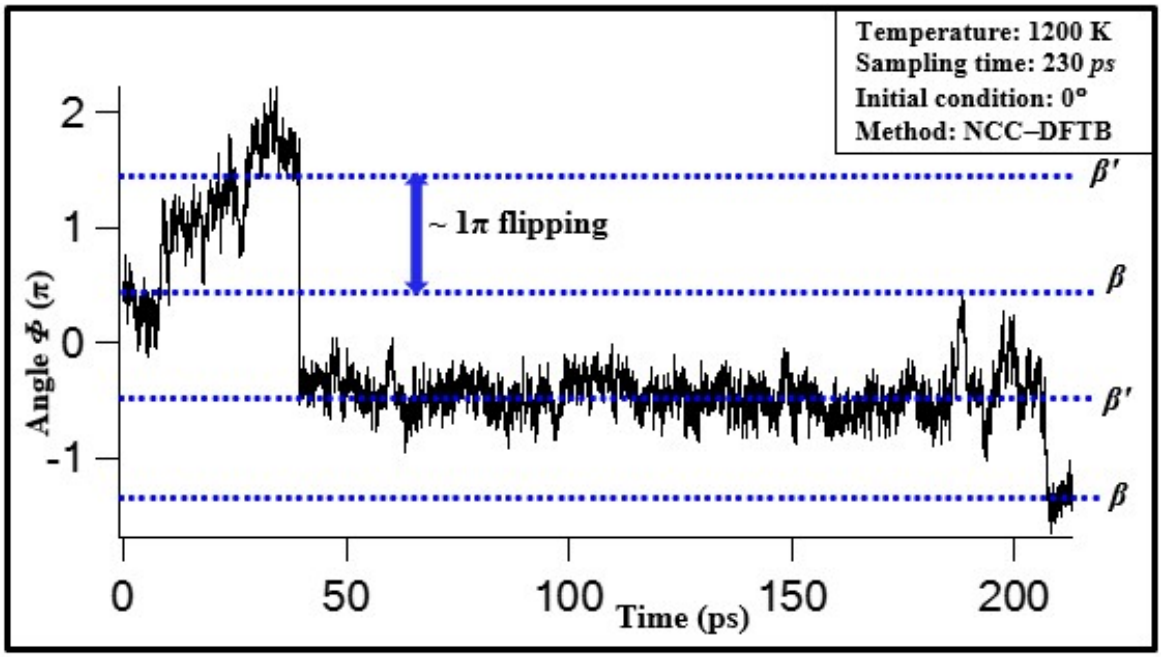


**Figure 2.** The NCC–DFTB/MD derived rotational trajectory (Dihedral angle $\phi$ (π) vs Time (ps)) of the diflourophenylene (compass needle) rotator at 1200K. The symbols $\beta$ and $\beta'$ represent the stable angular positions of the rotator as observed in the rotational potential energy surface of Figure (1).

$\beta \leftrightarrow \beta'$ flippings of the rotator of the crystalline molecular compass ROT–2F are not observed within the timeframe of currently run MD simulation (~200 ps timeframe was set due to being the present crystalline molecular assembly extremely giant and computationally expensive yet time consuming), the real–time flipping motion of it is genuinely observed at 1200 K. These observations at relatively higher temperature regime were not disclosed earlier by either of the theoretical or experimental techniques. The temporal dependence of the rotary trajectory is clearly seen in Figure 3 where the internal kinetic temperature of the ensemble is reduced to half (T = 600 K) from the previous T. At this temperature scale as well, the complete 1π flipping of the rotating segment from the position $\beta$ to $\beta'$ is observed, but the time required to exhibit this flipping is >250 ps (the initial velocities of every atomic nuclei of the unit cell are identical in both T); a relatively longer timeframe than that observed in T = 1200 K; which is quite obvious as the lower average kinetic temperature limits the magnitude of internal translational energy of the simulating particles of the microcanonical ensemble to the lesser extent and hence, requires a longer timeframe. The rotary profile depicts that the rotator stays at $\beta$ position for about 250 ps (average lifetime), and then turns into its 1π–flipped degenerate position $\beta'$ where it is found to reside for about 100 ps within the present simulation timeframe. The approximate net time consumed by the rotator to flip from $\beta$ position to $\beta'$ position ($\beta \rightarrow \beta'$ flipping) is observed as ~45 ps; more retarding flipping rates of the diflourophenylene rotator than that observed in T = 1200 K. Though the frequency of the flipping motions and the flipping rates of the rotator are observed to be slower, the exact angular positions $\phi$ and the internal alignments of the rotator (designated as $\beta$ and $\beta'$) inside the free–volume unit of the encompassing siloxaalkane spokes are reproduced well even when the average kinetic temperature T is lowered to 600K. As a whole, these NCC/DFTB–MD produced results at relatively high average kinetic temperature regimes confirmed the *Gaussian* run NCC/DFTB PES (*Gaussian*– external methodology) scanning techniques produced global minima structures B and B' of the present crystalline molecular compass ROT–2F and the respective degenerate flipping positions $\beta$ and $\beta'$ of its diflourophenylene rotator (Figure 1).

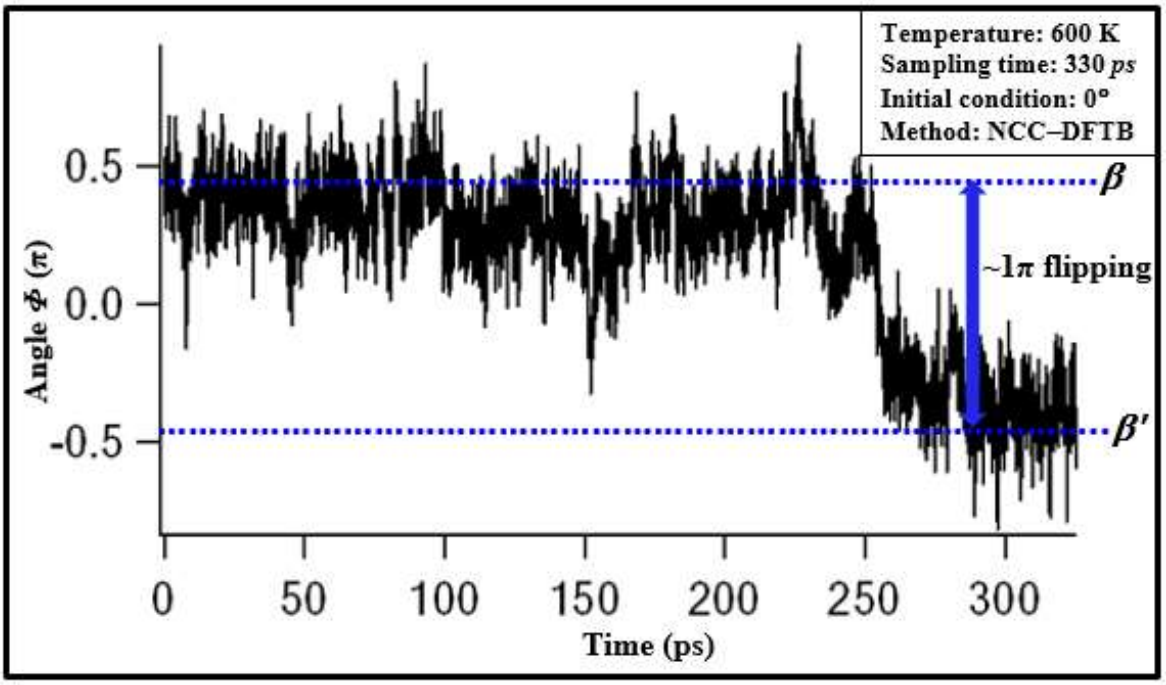


**Figure 3.** The NCC–DFTB/MD derived rotational trajectory (dihedral angle $\phi$ (π) vs Time (ps)) of the diflourophenylene (compass needle) rotator at 600 K. The symbols $\beta$ and $\beta'$ represent the stable angular positions of the rotator as observed in the rotational potential energy surface of Figure (1).

The rotary trajectories at relatively low average kinetic temperature regimes (T = 300 K and 273 K) are shown in Figure 4 and Figure 5 respectively where the frequent flipping motions of the rotator are not observed unlike at high temperature regimes. More particularly, at T = 300 K, the rotary trajectory (rotator) remains at the position $\beta$ for about 55 ps before undergoing a complete 1π flipping to the new position $\beta'$ where the rotator is found to spend for about 15 ps, and turns anticlockwise 2π rotation ($\beta' \leftrightarrow \beta'$) subsequently. After this absolute negative 2π rotation, the rotator remains completely unflipped even up to 80 ps within the limit of current simulation timeframe. The closed observation of the flipping time range consumed by the rotator at the same average kinetic temperature exemplifies the tentative flipping rate as ≅ 25 ps per 1π flipping ($\beta \rightarrow \beta'$); a rate slower than that observed at T = 1200 K (the flipping rate ≅ 8 ps/1π flip) for the same type flipping (the initial velocities of all atomic nuclei of the unit cell were derived randomly from the '*VelocityVerlet{}*' random seeding techniques, and were non-identical to those used for T = 600

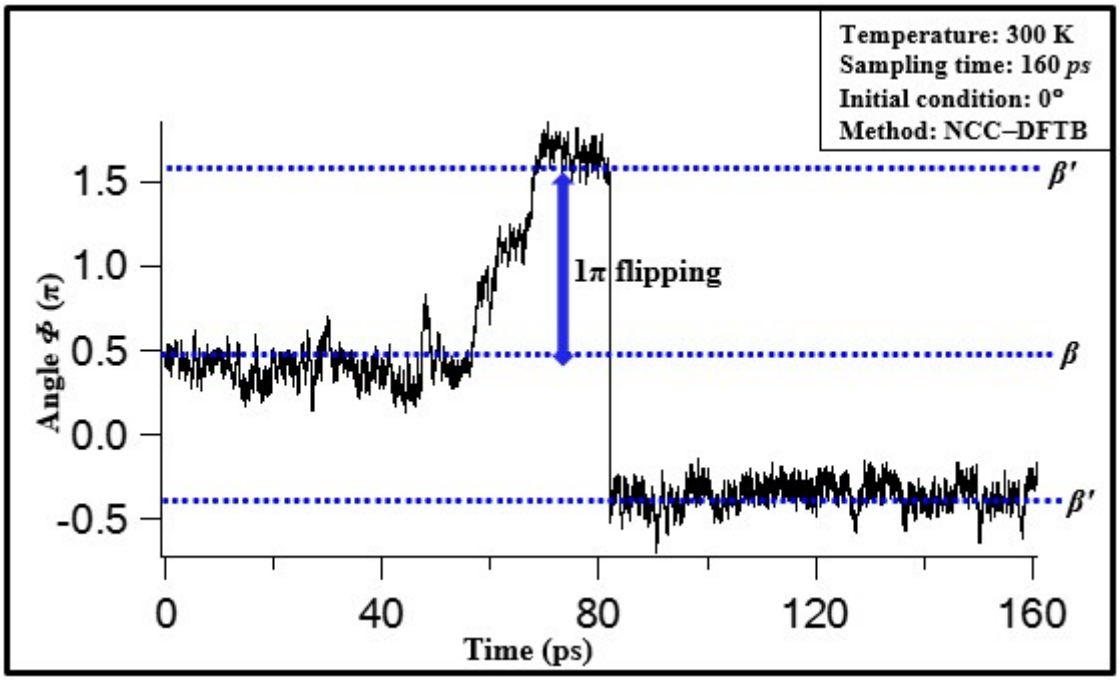


**Figure 4.** The NCC–DFTB/MD derived rotational trajectory (dihedral angle $\phi$ (π) vs Time (ps)) of the diflourophenylene (compass needle) rotator at 300 K. The symbols $\beta$ and $\beta'$ represent the stable angular positions of the rotator as observed in the rotational potential energy surface of Figure (1).

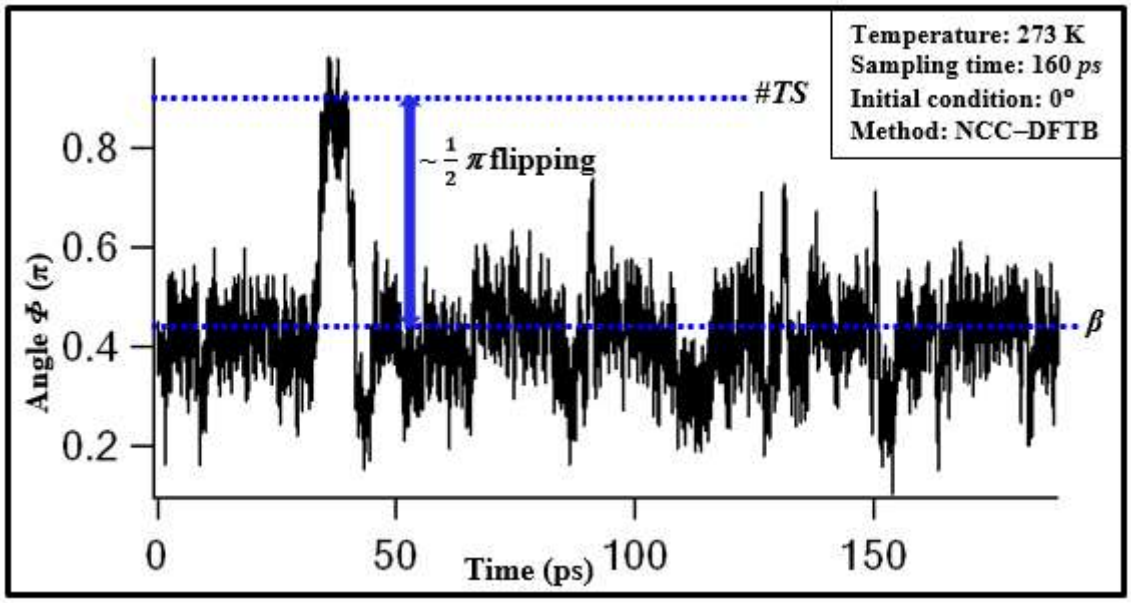


**Figure 5.** The NCC–DFTB/MD derived rotational trajectory (dihedral angle $\phi$ (π) vs Time (ps)) of the diflourophenylene (compass needle) rotator at 273K. The symbols *#TS* and $\beta$ represent the transition state and the global minimum state (stable angular positions) of the rotator as observed in the rotational potential energy surface of Figure (1).

K cases). This finding of the significantly slower rate is very much acceptable in terms of the average energy gained by the entire ensemble at low temperature as energetic as 298 K (room temperature at Kelvin scale): the lower average kinetic temperature always contributes less to the internal translational molecular energy of the simulating molecules than that induced internally by the relatively higher temperatures. When the average kinetic temperature is further lowered to 273 K (less than the room temperature at Kelvin scale), the rotary trajectory seems unable to switch its angles owing to the complete $\beta \rightarrow \beta'$ flipping. It means, within the present simulation timeframe (~200 ps), the rotary segment diflourophenylene is unable to overcome the energy barrier $E_a$ of the magnitude 4.9 kcal/ mol exists in between its two degenerate stable minima $\beta$ and $\beta'$ related to each other by 1π angular flip. Though the rotary pathway is slightly shifted to the position $\phi$ = 0.95π (a position near to the transition state #TS of the rotational PES (Figure 1)) after about 35 ps of the MD run, it immediately returns to the original position $\beta$. This angular change of the rotator is just recognized as its $\sim \frac{1}{2}\pi$ flipping, but the complete $\beta \rightarrow \beta'$ flipping of it is prevented due to the obstructions caused by the internal energetic barrier $E_a$. If the author was able to run this low temperature simulation for a relatively longer timeframe, the rotator could undergo 1π $\beta \rightarrow \beta'$ flipping as reported experimentally elsewhere [9], however, this analogy is practically infeasible not only due to being the current simulation assembly (crystalline molecular arrays) extremely complex (number of molecules/unit cell = 2; number of atoms/molecule = 195) but also due to bearing the extreme computational costs, optimum employments of the computational resources/disk space, and the most tedious mathematical iteration procedures.

In order to interpret qualitatively the effects of the substituents (in this case, F atoms) and size of the rotary segments encapsulated into the exactly same and chemically equivalent types peripheral siloxaalkane spokes, the author has presented a part of the NCC–DFTB/MD derived rotary profiles (timeframe ≤ 20 ps) computed for the both ROT–2F molecular compass and ROT–2H molecular gyroscope at the average kinetic temperatures of T = 1200 K and 600 K as shown in Figure 6 and Figure 7 respectively. Since the former crystalline molecular compound ROT–2F (orthorhombic crystal at 273 K) possesses a heavier rotary segment (ortho and meta F substituted diflourophenylene unit) whereas the latter crystalline compound ROT–2H (monoclinic crystal at 223 K) possesses an unsubstituted phenylene unit centrally, the time dependent rotary trajectories of their ratators (Figure 6 and Figure 7) depict distinct variations in the angular switching of the latter within the identical simulation timeframe of 20 ps at T = 1200 K and 14 ps at T = 600 K. Even though the exact angular positions of ROT–2F's and ROT–2H's rotating segments, and their two & three stable flipping positions within the angular frame of 1π (ROT–2F ($E_a$ = 4.9 kcal/mol) and ROT–2H ($E_a$ = 1.2 kcal/mol)) were projected beforehand by the PES scanning techniques (*Gaussian–external*), probing deep into the initial responses of their rotators to the internally induced average kinetic temperatures cum energies depicts the size dependency of them qualitatively. As shown in Figure 6, if the angular flow of the MD trajectories of ROT–2F and ROT–2H at average kinetic temperature T = 1200 K are compared, the bulkier diflourophenylne rotator of the former is found to remain unflipped but the lighter unsubstituted phenylene rotator of the latter shows both clockwise and anticlockwise flipping motions. Alike to this observation, the rotary profiles show an exactly same behavior when the kinetic temperature is reduced to T = 600 K (Figure 7); the contrasting angular flipping motions shown by the lighter rotator are clearly marked there itself. These responses of the light and bulky rotators to the internally induced average kinetic energy forecast the occurrence of relatively facile and restricted flipping motions of the ROT–2H molecular gyroscope and ROT–2F molecular compass respectively as observed experimentally in crystalline state.

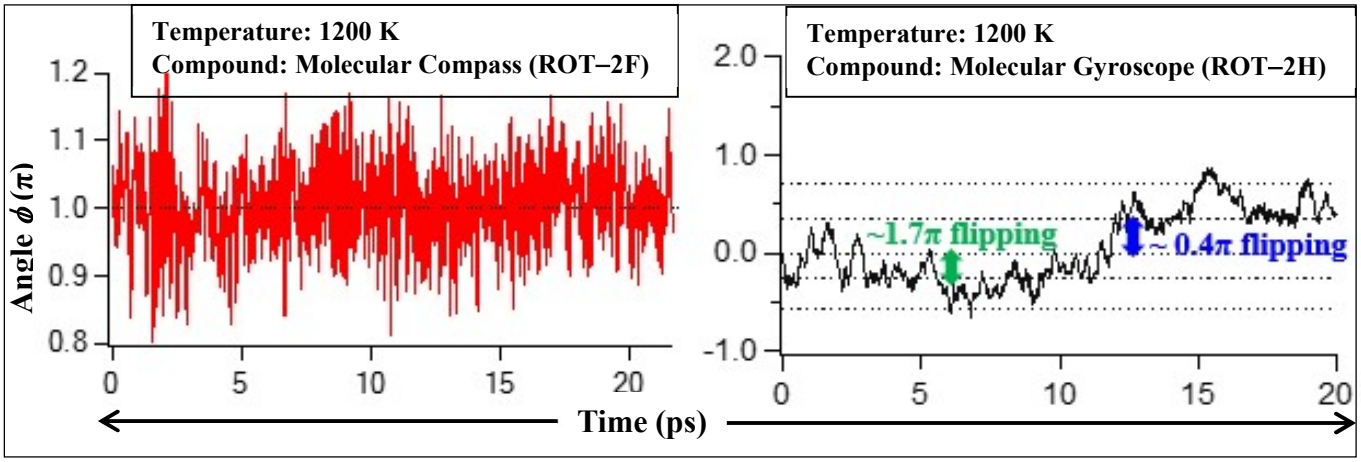


**Figure 6.** The NCC–DFTB/MD derived rotational trajectories (dihedral angle $\phi$ (π) vs Time (ps)) of the diflourophenylene (ROT–2F; Molecular compass) and phenylene (ROT–2H; Molecular gyroscope) rotators at kinetic temperature T = 1200K. These trajectories for short timeframe of 20ps were extracted just to compare their temporal flipping motions.

In conclusion, the NCC–DFTB/MD derived temporal rotary profiles of the dipolar diflourophenylene rotator of the present crystalline molecular compass ROT–2F at four different average kinetic temperature regimes (T = 1200 K, 600 K, 300 K, and 273 K) demonstrated the approximate lifespan of the latter at each of its stable minima $\beta$ and $\beta'$, and its flipping dynamics in real time scales. When the average kinetic temperature T is 1200 K, the frequent flipping motions of this dipolar rotator are observed, but when the T is reduced to lower temperature regimes such as T = 600 K, 300K, and 273K, the flipping dynamics is found to be retarded. At T = 1200 K, the rotator is found to consume tentative timescale of ≅ 8 ps for undergoing 1π $\beta \rightarrow \beta'$ flipping but at T = 600 K, around ≅ 45 ps is needed for the exactly same type flipping despite utilizing the similar initial velocities and atomic positions of every atomic nuclei of the unit cell structure as MD simulation input codes. When the average kinetic temperature is furthermore reduced to the scale of room temperature such as T = 300 K, the rotating segment is observed to switch its angular position from $\beta$ to $\beta'$ after the time gap of 55 ps, and is found to consume ≅ 25 ps per 1π flipping ($\beta \rightarrow \beta'$) (the initial velocities of all atomic nuclei

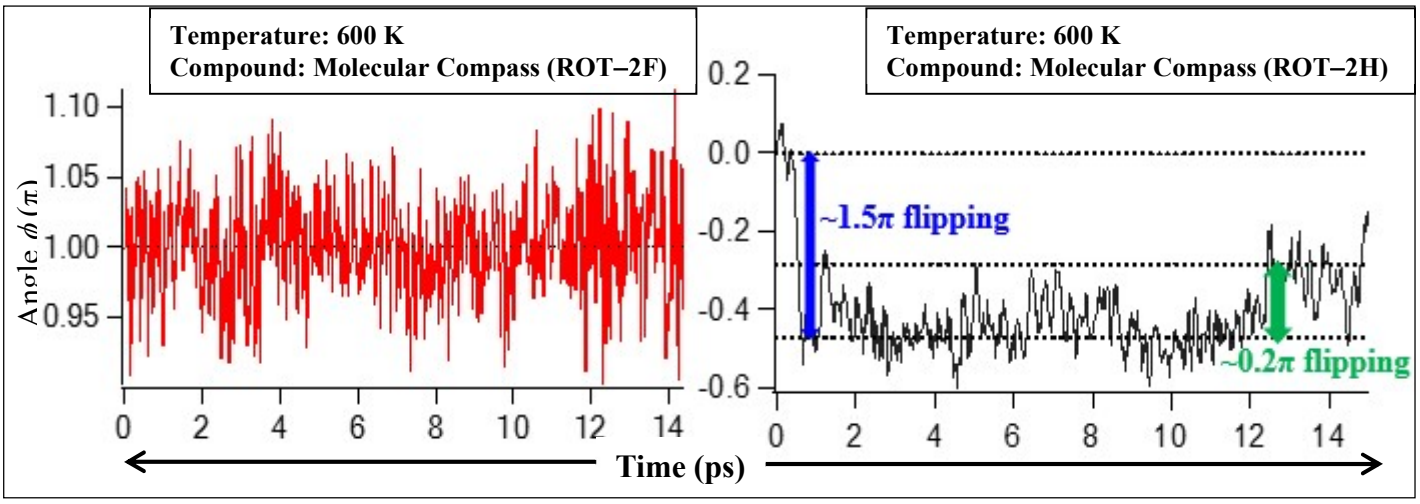


**Figure 7.** The NCC–DFTB/MD derived rotational trajectories (Dihedral angle $\phi$ (π) vs Time (ps)) of the diflourophenylene (ROT–2F; Molecular compass) and phenylene (ROT–2H; Molecular gyroscope) rotators at kinetic temperature T = 600K. These trajectories for short timeframe of 14ps were extracted just to compare their temporal flipping motions.

of the unit cell were derived randomly from the '*VelocityVerlet{}*' random seeding techniques, and were non-identical to those used for T = 1200 K and T = 600 K cases). This flipping is completely forbidden even up to 200 ps of the MD run when the average kinetic temperature T is decreased to the scale of T = 273 K; a lower temperature than the $T_{room}$ (= 298 K). It assures that the average internal kinetic energy that the simulating ensemble gained at T = 273 K is not enough to overcome the flipping barrier $E_a$ exists in between $\beta$ and $\beta'$. Even though the rotary trajectory seems to be shifted towards the angular position as equal as 0.95π from the initial position $\beta$ ($\phi$ = 0.44π), it only reaches closer to the transition state #TS but is unable to cross the same readily. This analogy might be insignificant if the present author was able to extend the MD simulation timescale to >200 ps which was however, practically not viable based on the computational resources and disk spaces occupied by the current giant sized molecular ensembles in the course of implementing their complex iterative quantum mechanical procedures genuinely. As a whole, all these DBTB+/MD simulation derived temperature dependent rotary profiles verified the experimentally observed temperature dependent flipping dynamics of the dipolar rotator of the crystalline molecular compass ROT–2F with completely closed structural topology quantitatively in real time scales. These justifications and quantum mechanical interpretations seriously promote the extraordinary computing abilities of the DBTB+/MD simulation package, and its standalone, versatile quantum mechanical applications in the light of incorporating long-ranged non-bonding interactions, implementing the entire computational iterative procedures efficiently by addressing the rigorous roles of the Mulliken charges along with offering two order faster simulation rates than that of the typical DFT scheme.

### 3.3 Determination of Rotational Energy Barrier $E_a$ from Real–Time Flipping Dynamics

In order to validate the PES scanning technique (*Gaussian–external*) derived rotational energy barrier $E_a$, the author has employed the final pre–exponential factor $A$ (Arrhenius constant) eliminated form of the Arrhenius equation as shown in eq. (1), and utilized the NCC–DFTB/MD derived flipping rates $\kappa_1$ and $\kappa_2$ at two different average kinetic temperatures.

$$\ln\left[\frac{\kappa_1}{\kappa_2}\right] = -\frac{E_a}{K_B}\left[\frac{1}{T_1} - \frac{1}{T_2}\right] \quad (1)$$

Where;

$\kappa_1$ = flipping rate at $T_1$ = 1200 K

$\kappa_2$ = flipping rate at $T_2$ = 600 K

$E_a$ = flipping energy barrier

$K_B$ = Boltzmann constant ($1.987\times10^{-3}$ kcal mol$^{-1}$ K$^{-1}$).

Since, within the MD simulation timeframes implemented by the present author, the complete yet stable 1π flipping motions of the dipolar diflourophenylene rotator of the crystalline molecular compass ROT–2F with relatively more lifespans at $\beta$ (structure B) and $\beta'$ (structure B') positions are distinctly observed at high average kinetic temperature regimes of T = 1200 K and T = 600 K. Therefore, the respective flipping rates $\kappa_1$ and $\kappa_2$ were determined from their MD trajectories based on the total time consumed by the rotator for exhibiting a complete 1π $\beta \rightarrow \beta'$ flipping. The $\kappa_1$ and $\kappa_2$ were estimated as 0.125 ps$^{-1}$ and 0.022 ps$^{-1}$ at 1200 K and 600 K respectively. The significantly slower flipping rate at lower temperature range is very much convincible as the internally induced average kinetic energy equivalent to that temperature scale of the simulating atomic nuclei of the entire ensemble is lower than that attained at higher temperature regime. While substituting those $\kappa_1$ and $\kappa_2$ in eq. 1, the rotational energy barrier $E_a$ is found as 4.3 kcal/mol; a reasonable value to that of the $E_a$ (= 4.9 kcal/mol) determined through the *Gaussian–external* based PES scanning technique (Figure 1). Thus estimated yet quite validated $E_a$ value further marks the extreme potentiality of the NCC–DFTB/MD scheme in simulating computationally complex crystalline molecular systems despite suffering from the approximate, quantum mechanically less competent mathematical formulations designed for addressing the predominant effects of the long-ranged molecular interactions existing throughout the molecular crystals that are morphologically as equivalent as the present ROT–2F crystalline molecular compass systems. The DFTB+ scheme recently assured theses competencies by incorporating the self-consistent charge SCC approach into its iterative computational procedures, which is however, impracticable to be employed in simulating the complex crystalline molecular systems under its simulation parser codes [2, 14, 19].

## 4. CONCLUSION

The primary objective of this research work was to investigate the real–time flipping dynamics of the macroscopic compass like molecular arrays of the crystalline macrocyclic compound ROT–2F: each molecule possesses a dipolar diflourophenylene unit encompassed externally by the Si–C spin axis linked –Si– & –Si–O– made three explicit siloxaalkane framework. As per the X–ray and $^1$H– NMR analytical techniques based experimental observations, this siloxaalkane molecular compass was found to behave as an amphidynamic crystalline material at temperature T = 273 K: the central dipolar diflourophenylene unit (compass needle) undergoes a complete 1π flipping with two degenerate positions $\beta$ and $\beta'$ on its Si–C spin axis while the every peripheral siloxaalkane arm remains fully static. Owing to such type amphidynamic features and many other experimentally reported promising nanotechnological and molecular machinery attributes of this molecular compass in nanoscale science, present author was triggered very much towards revealing its promising yet functionalizable physicochemical properties and indispensable dynamical assets by employing the computationally efficient yet potent DFTB+ schemes (SCC and NCC approaches). The *Gaussian–external* methodology drove DFTB methods, and the DFTB techniques alone probed in-depth structural characterizations and molecular energetics were already reported. In the present contribution, many experimentally unpredicted yet impossible rotary dynamical descriptors such as temporal rotary profiles, time dependent flipping dynamics and kinetics, life spans of the rotator at each of its intermittent low energy yet degenerate stable positions ($\beta$ and $\beta'$), flipping barrier $E_a$ that the diflourophenylene rotator is supposed to overcome, etc. were theoretically computed by employing the NCC–DFTB based molecular dynamics (MD)

simulation technique. Besides these, the temporal behavior of this dipolar rotating segment plus the closely correlated structural morphology and its descriptive parameters were theorized.

Generally, the NCC–DFTB/MD produced rotary trajectories at high average kinetic temperature regimes T = 1200 K and T = 600 K clearly displayed the 1π $\beta \rightarrow \beta'$ flipping at the specific angular positions identical to those predicted through the *Gaussian* run NCC–DFTB method (*Gaussian–external*) based potential energy surface (PES) scanning techniques. The rotator showed significantly longer lifespans at each of its stable equilibrium positions $\beta$ and $\beta'$ before undergoing any sorts of the clockwise/anticlockwise type 1π $\beta \leftrightarrow \beta'$ flippings within the simulation timeframe adopted throughout this study. In particular, at T = 1200 K, the rotator was found to consume tentative timescale of ≅ 8 ps for undergoing a complete 1π $\beta \rightarrow \beta'$ flipping but at T = 600 K, it required ≅ 45 ps. When that T of the simulating ensemble was furthermore lowered to the scale of room temperature ($T_{room}$ = 298 K) such as T = 300 K, the rotating segment was observed to switch its angular position from $\beta$ to $\beta'$ only after about 55 ps of the MD run, and found to consume ≅ 25 ps for the same type flipping. This flipping motion was completely forbidden even up to 200 ps of the MD run when the T was again decreased to the scale of 273 K; specifying that no simulation ensemble (crystalline assembly) was able to gain the average kinetic energy (equivalent to 273 K) required by its molecular entity for overcoming the flipping barrier of magnitude $E_a$ = 4.9 kcal/mol exists in between its two global minima $\beta$ and $\beta'$. Unlike these interpretations carried out at variable temperature regimes, the rotary motions of the two differently sized rotators (light rotator: phenylene (molecular gyroscope ROT–2H), and bulky rotator: diflourophenylene (molecular compass ROT–2F)) encapsulated into the chemically identical siloxaalkane static frameworks were inspected individually at the same kinetic temperature regime in order to compare their responses towards the induced temperature scales and flipping propensities in real time. The contrasting angular switching of them with the few notable yet facile frequent flipping motions of the former rotator were distinctly observed at both of the kinetic temperatures: T =1200 K, and T = 600 K. Moreover, the NCC–DFTB/MD derived temporal rotary profiles were used to approximate the flipping energy barrier $E_a$ by employing the final pre-exponential factor $A$ (Arrhenius constant) eliminated form of the Arrhenius equation wherein the corresponding MD predicted flipping rates $\kappa_1 = 0.022\ ps^{-1}$ and $\kappa_2 = 0.125\ ps^{-1}$ were substituted. Thus determined energetic magnitude of the $E_a$ = 4.3 kcal/mol was found to be in quite agreeable range to that computed through the *Gaussian – external* PES scanning techniques ($E_a$ = 4.9 kcal/mol). In conclusion, all the aforementioned theoretical interpretations concentrated into the computationally complex crystalline molecular systems justified well the remarkable computing efficiencies of the NCC–DFTB/MD simulation scheme, and its standalone, versatile quantum mechanical applications despite its weakness in approximating mathematical formulations and modeling the entire simulation parser codes. To the experiences of the present author, more competent yet precise results could be achieved if the SCC approaches of the DFTB can be implemented genuinely even though it demands more computational disk space and memories while implementing its entire quantum mechanical formulations stepwise.

**ACKNOWLEDGEMENT**

The entire real–time flipping motions and the associated picosecond flipping dynamics of the dipolar diflourophenylene rotator of the crystalline siloxaalkane molecular compass ROT–2F presented throughout this research article were based on the calculations carried out with the high performance computing systems available at Theoretical Chemistry Laboratory, Graduate School of Science, Tohoku University, Sendai, Miyagi, Japan. An emeritus Professor Hirohiko Kono of the same laboratory is acknowledged for the constructive criticisms.

**COMPETING INTEREST**

Author has declared that no competing interests exist.

**REFERENCES**

[1]. Marahatta AB. *Gaussian–External* Methodology Predicted Crystal Structures, Molecular Energetics, and Potential Energy Surface of the Crystalline Molecular Compass. Asian Journal of Applied Chemistry Research. 2023; 14(1):8–25.

[2]. Available: https://journalajacr.com/index.php/AJACR/article/view/255

[3]. Marahatta AB. Performance Evaluation of DFTB1 and DFTB2 Methods in Reference to the Crystal Structures and Molecular Energetics of Siloxaalkane Molecular Compass. International Journal of Progressive Sciences and Technologies. 2023; 14(1):12–31.

[4]. Available: https://ijpsat.org/index.php/ijpsat/article/view/5631

[5]. Balzani V, Venturi M, Credi A. Molecular Devices and machines: A Journey into the Nano World; Wiley-VCH: Weinheim, Germany, 2003.

[6]. Kelley TR. Molecular Machines. Topics in Current Chemistry, Springer, Berlin, Heidelberg, New York, 2005.

[7]. Dominguez Z, Dang H, Strouse MJ, Garcia-Garibay MA. Molecular "compasses" and "gyroscopes." III. Dynamics of a phenylene rotor and clathrated benzene in a slipping-gear crystal lattice. Journal of American Chemical Society. 2002; 124(26):7719–7727.

[8]. Available: https://pubmed.ncbi.nlm.nih.gov/12083925/

[9]. Horansky RD, Clarke LI, Price JC, Karlen SD, Jarowski PD, Santillan R, Garcia-Garibay MA. Dipolar rotor-rotor interactions in a difluorobenzene molecular rotor crystal. Physical Review B. 2006; 74:054306(1–12).

[10]. Available: https://journals.aps.org/prb/abstract/10.1103/PhysRevB.74.054306

[11]. O'Brien ZJ, Natarajan A, Khan S, Garcia-Garibay MA. Synthesis and Solid-State Rotational Dynamics of Molecular Gyroscopes with a Robust and Low Density Structure Built with a Phenylene Rotator and a Tri(meta-terphenyl)methyl Stator. Crystal Growth & Design. 2011; 11(6): 2654–2659.

[12]. Available: https://pubs.acs.org/toc/cgdefu/11/6

[13]. Setaka W, Ohmizu S, Kabuto C, Kira M. A Molecular Gyroscope Having Phenylene Rotator Encased in Three-spoke Silicon-based Stator. Chemistry Letters. 2007; 36(8), 1076–1077.

[14]. Available: https://academic.oup.com/chemlett/article-abstract/36/8/1076/7386255?redirected From=fulltext

[15]. Setaka W, Ohmizu S, Kira M. Molecular Gyroscope Having a Halogen-substituted *p*-Phenylene Rotator and Silaalkane Chain Stators. Chemistry Letters. 2010; 39(5), 468–469.

[16]. Available: https://academic.oup.com/chemlett/article/39/5/468/7387984

[17]. Setaka W, Yamaguchi K. Thermal modulation of birefringence observed in a crystalline molecular gyrotop. The Proceedings of the National Academy of Sciences. 2012; 109(24), 9271–9275.

[18]. Available: https://www.pnas.org/doi/full/10.1073/pnas.1114733109

[19]. Akimov AV, Kolomeisky A. Dynamics of Single-Molecule Rotations on Surfaces that Depend on Symmetry, Interactions, and Molecular Sizes. Journal of Physical Chemistry C. 2011; 115(1), 125–131.

[20]. Available: https://pubs.acs.org/doi/abs/10.1021/jp108062p

[21]. Marahatta AB, Kanno M, Hoki K, Setaka W, Irle S. Theoretical Investigation of the Structures and Dynamics of Crystalline Molecular Gyroscopes. Journal of physical chemistry C. 2012; 116, 4845−24854.

[22]. Available:https://journals.scholarsportal.info/details/19327447/v116i0046/24845tiotsadocmg.xml

[23]. Marahatta AB, Kono H. Comparative Theoretical Study on the Electronic Structures of the Isolated Molecular Gyroscopes with Polar and Nonpolar Phenylene Rotator. International Journal of Progressive Sciences and Technologies. 2020; 20(1):109–122.

[24]. Available: https://ijpsat.org/index.php/ijpsat/article/view/1716

[25]. Marahatta AB, Kono H. SCC−DFTB Study for the Structural Analysis of Crystalline Molecular Compasses. Chemistry Research Journal. 2022; 7(4):77−94.

[26]. Available:chrome-extension://efaidnbmnnnibpcajpcglclefindmkaj/https://chemrj.org/downlo ad/vol-7-iss-4-2022/chemrj-2022-07-04-77-94.pdf

[27]. Marahatta AB, Kono H. Structural Characterization of Isolated Siloxaalkane Molecular Gyroscopes via DFTB-based Quantum Mechanical Model. International Journal of Progressive Sciences and Technologies. 2021; 26(1):526−541.

[28]. Available: https://ijpsat.org/index.php/ijpsat/article/view/2950

[29]. Marahatta AB. DFTB1 and DFTB2 Based Real−Time Flipping Motion Studies of Central Phenylene Rotator of Crystalline Siloxaalkane Molecular Gyroscope. International Journal of Progressive Sciences and Technologies. 2024; 42(2):19−39.

[30]. Available: https://ijpsat.org/index.php/ijpsat/article/view/5732/3700

[31]. Elstner M, Hobza P, Frauenheim T, Suhai S, Kaxiras E. Hydrogen bonding and stacking interactions of nucleic acid base pairs: a density-functional-theory based treatment. Journal of Chemical Physics. 2001; 114:5149−5155.

[32]. Available:https://pubs.aip.org/aip/jcp/article-abstract/114/12/5149/183912/Hydrogen-bondi ng-and-stacking-interactions-of?redirectedFrom=fulltext

[33]. (a) Verlet L. Computer "Experiments" on Classical Fluids. I. Thermodynamical Properties of Lennard-Jones Molecules. Physical Review. 1967; 159:98−103.

[34]. Available: https://journals.aps.org/pr/pdf/10.1103/PhysRev.159.98

[35]. (b) Verlet L. Computer "Experiments" on Classical Fluids. II. Equilibrium Correlation Functions. Physical Review. 1968; 165:201−214.

[36]. Available: https://journals.aps.org/pr/abstract/10.1103/PhysRev.165.201

[37]. DFTB$^+$ Version 1.3 User Manual.

[38]. Available: https://dftbplus.org/fileadmin/DFTB-Plus/public/dftb/current/manual.pdf